energies

Review

A Survey on Load Frequency Control of Multi-Area Power Systems: Recent Challenges and Strategies

Xinghua Liu [1], Siwei Qiao [1] and Zhiwei Liu [2,3,*]

[1] School of Electrical Engineering, Xi'an University of Technology, Xi'an 710048, China
[2] School of Automation, Huazhong University of Science and Technology, Wuhan 430074, China
[3] Key Laboratory of Image Processing and Intelligent Control of Education Ministry of China, Wuhan 430074, China
* Correspondence: zwliu@hust.edu.cn

Abstract: Load frequency control (LFC) is well known for balancing the load demand and frequency for a multi-area power system. Studies have proven that LFC can improve the global performance of multi-area power systems. In recent years, the increasing proportion of renewable energy, integration of EVs, and cyber-attacks have become the main challenges in LFC power systems. Different strategies have been applied in the literature for LFC power systems and the possible impacts of renewable energy, EVs, and cyber-attacks. This survey paper is devoted to the research on directions in LFC multi-area power systems. The mathematical model of recent challenges in LFC multi-area power systems is summarized and the similarities and differences of these challenges are analyzed. The uncertainty of renewable energy is a frequently noted issue in LFC power systems; however, the uncertainty that exists in controller design is often ignored. In this survey, we analyze methods for treating the uncertainty of renewable energy and controller. This survey paper introduces the most recent research on LFC and acquaints anyone interested in its development, such that the most effective strategies can be developed by the researchers.

Keywords: power system; LFC; renewable energy; cyber-attacks; sliding mode control; data-driven

Citation: Liu, X.; Qiao, S.; Liu, Z. A Survey on Load Frequency Control of Multi-Area Power Systems: Recent Challenges and Strategies. *Energies* **2023**, *16*, 2323. https://doi.org/10.3390/en16052323

Academic Editor: Abu-Siada Ahmed

Received: 20 January 2023
Revised: 23 February 2023
Accepted: 24 February 2023
Published: 28 February 2023

1. Introduction

Recently, social development and population growth have caused the demand for energy support to grow gradually. To guarantee the supply of power, the requirements for the power system are becoming higher and higher. Due to the steadily escalating size and intricacy of modern power systems [1], the problems and challenges that the power system may encounter can be expected to increase as well. Load frequency control (LFC) is widely used to judge whether the power system is in normal operation [2–5]. In practice, the valve opening of the governor is controlled by LFC, in which the control signal is made up of the frequency deviation. The volume of steam flow into the steam turbine changes when the real-time frequency deviates from the steady value. The frequency of the power generator is regulated to a steady value by controlling the rotor speed [6]. In a power system, LFC has been proven to effectively maintain the frequency and power flow of tie-lines between areas.

With increasing demand for electric power, the pressure on the power system is greatly increased. In ongoing research, scientists have realized that renewable energy is one of the best choices to lighten the power supply pressure of the traditional power system [7–11]. Environmental damage (e.g., climate change) caused by crude oil and fossil fuels is increasing the dependence on cleaner renewable energy. Normally, renewable energy includes solar, biomass, wind, hydro, and wave power. Among renewable energy resources, solar and wind power have been the most considered in relieving pressure on energy demand over the last few years. To maximize the utilization of renewable resources, more and more academics are placing their focus on these areas and intensifying research into them.

In [12], a wind farm and photovoltaic (PV) model was integrated with an LFC power system. The LFC problem of multi-area wind power systems involving the communication delay was investigated in [13]. In [14], the LFC problem was investigated by considering the output wind power fluctuation for a significant wind power penetration time-delay power system. In [13], a fuzzy logic integral sliding mode controller was proposed for multi-area wind power systems. A new model was developed to explore the influence of the LFC power system frequency fluctuation on the PV output power in [15]. In [16], diesel generators, PVs, and wind turbines were considered as a multi-source power system, and LFC techniques were applied to balance the frequency and multi-source electricity. As the share of renewable energy in the power system increases, the system inertia is constantly reduced, which impacts system stability, leading to frequency deviations [17]. Based on a dual-structured fuzzy (DSF) model, a proportional and integral switched controller was proposed in [18] to improve the frequency regularization of the μ-grid integrated with wind power. In [19], a fractional-order PID was developed for a multi-sources interconnected renewable power system. In [20], a non-conventional quasi-oppositional dragonfly algorithm was used to find the optimal parameters of the PID controller in the LFC renewable power system. Persistent large deviations in tie-line power exchange and system frequency in an LFC power system are harmful to appliances, can lead to instability of operation, reduce the lifetime of connected devices, and even result in a crash of the power system.

In addition to the above challenges, battery energy storage units are integrated into modern power systems. Due to the penetration of renewable energy into power grids, frequency fluctuations can be highly disturbed. Battery energy storage units can smooth these fluctuations, enhancing the transient response of the power system. This process is carried out through a continuous bidirectional power flow between the battery energy storage unit and the grid [21]. In [22], a battery energy storage unit was connected to a wind power system, reducing the adverse effects of frequency deviations. Today, batteries are widely applied in electric vehicles (EVs), and research attention has become focused on issues related to EVs. In [21], a modern power grid was constructed with generators, photovoltaic, solar thermal, wind, and energy storage for study of the LFC issue. EVs play an essential role in low-carbon development, and have significant implications for power grids. The adoption of EVs can effectively improve the power grid's load factor and reduce the electricity supply cost [23]. To make the LFC problem more realistic, a hybrid power system (conventional thermal, electric vehicle (EV), and solar thermal) was considered in [16].

Open communication networks are used in LFC power system signals transmission [3]. Unfortunately, safety and other issues are gradually becoming more serious due to the openness of this network. Cyber-attacks on communications networks can impact the operation of power systems, potentially leading to serious disruptions [24]. A frequency fluctuation due to load change or cyber-attack in one area may spread to all connected neighboring areas and deal further damage to overall power system stability. The use of a communication network is vulnerable to different types of hostile attacks generated by adversaries. In LFC power systems, the most widely considered cyber-attacks are deception attacks and denial-of-service (DoS) attacks [24]. In [25], a handshake protocol was used to design event-triggered strategies and identify DoS attacks in an LFC power system. In [26], a switched system was constructed to analyze the stability of an LFC power system under DoS attacks and deception attacks. In [27], an event-triggered LFC mathematical model was constructed for a power system under deception attack. An event-based PI secure load-frequency controller was utilized for power systems suffering from deception attacks in [27]. To handle the significant wind power penetration and time-delay problem, a novel decentralized sliding-mode LFC strategy was designed for multi-area power systems in [14]. It can be seen from these studies that the challenges involved in integrating LFC with power systems are very important. Although renewable energy has many advantages and the network is convenient, the resulting stability issues for power systems cannot be ignored. To ensure the good performance of renewable power systems, various control strategies have been developed for the LFC issue. Figure 1 is shows the organization of the rest of this review paper.

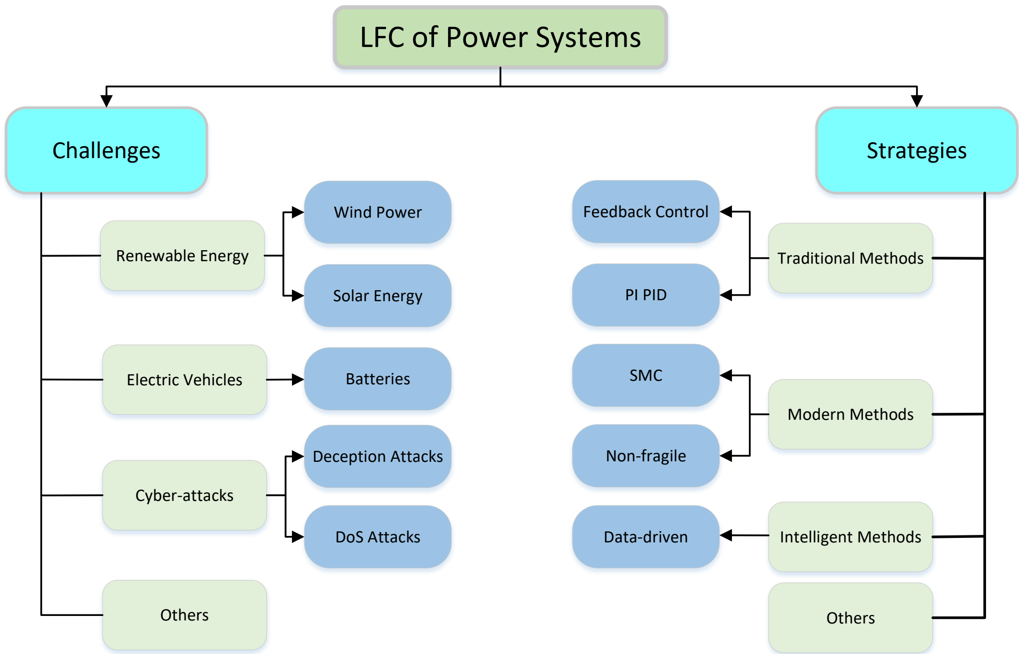

Figure 1. Organization of the paper.

In recent years, system control theory has been applied to solve the above-mentioned challenges in the power system [28]. In this survey, we mainly focus on the methods of traditional control, modern control, and intelligent control. Based on system control theory, many excellent control methods have been proposed for power systems to address various challenges. Table 1 describes the contributions and limitations of recent research papers on these challenges.

Table 1. Comparison of recent studies on LFC in the literature.

Wind Power	Solar Energy	EVs	Deception Attacks	DoS Attacks	Feedback Control	PI/PID	SMC	Non-Fragile	Data-Driven	
√	×	×	×	×	×	×	√	×	×	[13]
×	√	×	×	×	×	√	×	×	√	[29]
×	×	×	×	×	×	×	√	×	√	[30]
×	×	×	×	×	×	√	×	×	√	[31]
×	×	√	×	×	×	√	×	×	×	[32]
×	√	×	×	×	×	×	×	×	√	[33]
√	√	×	×	×	×	√	×	×	×	[16]
√	√	×	×	×	×	×	×	×	√	[28]
×	×	×	×	×	×	√	×	√	×	[34]
×	√	√	×	×	×	×	×	×	√	[21]
×	×	×	√	√	√	×	×	×	×	[35]
×	×	×	√	×	√	√	×	×	×	[27]
×	×	×	√	×	×	×	√	√	×	[36]
√	×	√	×	×	×	×	√	×	×	[9]
×	×	×	×	×	×	×	×	×	√	[37]
√	×	×	×	×	×	√	×	×	√	[38]

In this survey, we review LFC power systems, recent challenges, and the strategies used to address them. The main contributions are summarised in the following aspects:

1. This survey uses the flexible renewable power system model, in which the effect and uncertainty caused by renewable energy (wind and solar) are considered. Based

on the detailed description of different mathematical models of renewable energy, the LFC problem can be solved with high productivity.
2. Identifying types of cyber-attacks pertaining to LFC can help to formulate reasonable and effective strategies. We focus on the characteristics of these cyber-attacks and analyze their effects on LFC power systems.
3. By optimizing or integrating control methods, excellent control strategies can be obtained and control performance can be improved. Intelligent control is more effective in solving the LFC issue for power systems with multiple renewable energy sources or those under cyber-attack due to its advantages in processing large amounts of data.

The remainder of this article is outlined as follows. The basis of LFC power systems in terms of the mathematic model and state space function is explained in Section 2. Section 3 introduces recent challenges related to LFC power systems. Section 4 describes defensive methods based on different control strategies. Finally, Section 5 concludes the survey.

2. Power System Model for LFC

To show the mathematical relationship and signal transmission of an LFC power system, a simplified model is provided here. Usually, the overall power system consists of M control areas connected by tie-lines [3–5]. Figure 2 presents a simplified i-th area system model.

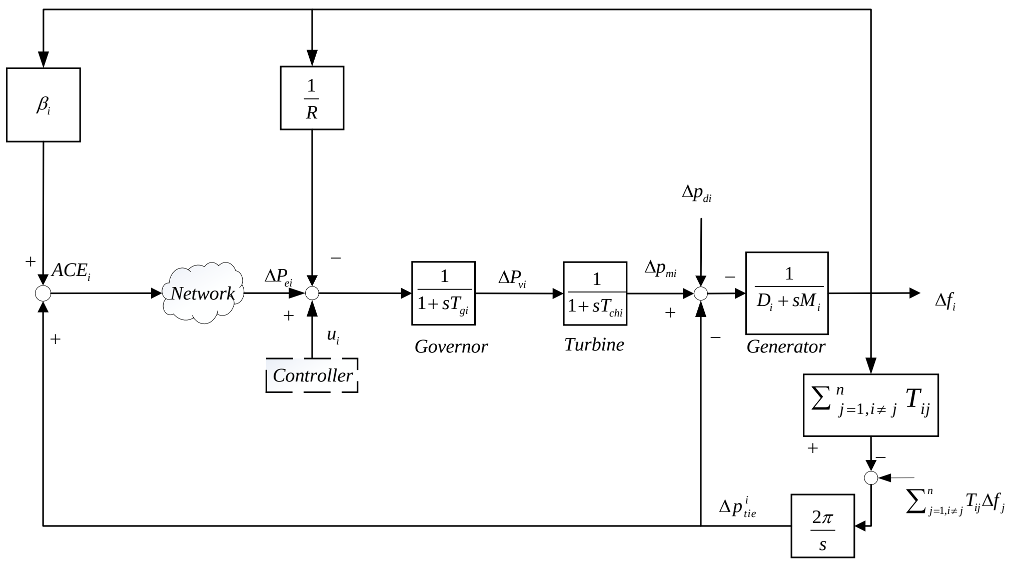

Figure 2. Simplified model of power system.

The power system is a huge and very complex control system. Mostly, simplified linear models [3–9] have been proposed to show the operation of the actual dynamics for the multi-area power system. Based on device relationship and signal transmission, the mathematical model is expressed as

$$\begin{cases} \Delta\dot{P}_{mi}(t) = -\frac{\Delta P_{mi}(t)}{T_{chi}} + \frac{\Delta P_{vi}(t)}{T_{chi}}, \\ \Delta\dot{P}_{tie}^{i}(t) = 2\pi \sum\limits_{j=1,i\neq j}^{n} T_{ij}(\Delta f_i(t) - \Delta f_j(t)), \\ \Delta\dot{P}_{vi}(t) = -\frac{\Delta f_i(t)}{R_i T_{gi}} - \frac{\Delta P_{vi}(t)}{T_{gi}} - \frac{\Delta P_{ei}(t)}{T_{gi}} + \frac{u_i(t)}{T_{gi}}, \\ \Delta\dot{f}_i(t) = \frac{\Delta P_{mi}(t)}{M_i} - \frac{D_i \Delta f_i(t)}{M_i} - \frac{\Delta P_{tie}^{i}(t)}{M_i} - \frac{\Delta P_{di}(t)}{M_i}, \\ ACE_i = \Delta P_{tie} + \beta_i \Delta f_i. \end{cases} \tag{1}$$

The nomenclature is summarised in Table 2.

Table 2. Nomenclature of the power system.

Parameters	Mean	Parameters	Mean
ΔP_{mi}	Generator power deviation	ΔP_{vi}	Control valve position deviation
ΔP_{tie}^{i}	Tie-line power exchange	Δf_i	Frequency deviation
ΔP_{ei}	Integral of ACE	ΔP_{di}	Load demand disturbance
β_i	Frequency deviation factor	D_i	Load damping coefficient
M_i	Rotational inertia of the generator set	ΔP_{di}	Load demand disturbancex
T_{chi}	Turbine time constant	R_i	Governor droop characteristic

We first define the following:
$x_i(t) = [\Delta P_{mi}, \Delta P_{vi}, \Delta P_{tie}^{i}, \Delta f_i]^\top$, $y_i(t) = ACE_i$.
Furthermore,

$$A_i = \begin{bmatrix} -\frac{1}{T_{chi}} & \frac{1}{T_{chi}} & 0 & 0 \\ 0 & -\frac{1}{T_{gi}} & 0 & -\frac{1}{R_i T_{gi}} \\ 0 & 0 & 0 & 2\pi \sum\limits_{j=1, j\neq i}^{n} T_{ij} \\ \frac{1}{M_i} & 0 & -\frac{1}{M_i} & -\frac{D_i}{M_i} \end{bmatrix}, \quad \begin{array}{l} B_i = \left[0, \frac{1}{T_{gi}}, 0, 0\right]^\top, \\ C_i = [0, 0, 1, \beta_i]^\top, \\ F_i = \left[0, 0, 0, -\frac{1}{M_i}\right]^\top. \end{array} \tag{2}$$

Thus, the wind power system state vector space function is represented as

$$\begin{cases} \dot{x}_i(t) = A_i x_i(t) + B_i u_i(t) + F_i w_i(t), \\ y_i(t) = C_i x_i(t), \end{cases} \tag{3}$$

where $u_i(t)$ is defined as the control input and $w_i(t) = \Delta P_{di}$ is the system disturbance, which is bounded satisfying $\Delta P_{di} < \epsilon$, where ϵ is a positive constant.

3. Descriptions of Challenges

3.1. Renewable Energy

With the development of the power system, power demands have gradually increased. Therefore, the renewable energy power system is presented to lighten this pressure.

3.1.1. Wind Power

Wind power is a primary source of renewable energy. However, two main negative effects appear in the LFC wind power system. The ability to balance inertia is reduced. The complexity of variation of generation and additional uncertainty is raised.

(1) The wind power system integrates a capacity wind turbine generator (WTG) with a modern power system [7–9]. The dynamic model of the WTG can be written as

$$\Delta \dot{P}_{WTGi} = \frac{1}{T_{WTGi}} \Delta P_{w-i} - \frac{1}{T_{WTGi}} \Delta P_{WTGi} \tag{4}$$

where P_{WTGi} is defined as the output power change of WTG, P_{w-i} represent the wind power, and T_{WTGi} is the time constant of WTG in the i-th area.

Therefore, the dynamic model of the i-th area wind power is represented as

$$\begin{cases} \dot{x}_{win}(t) = A_{win} x_{win}(t) + B_{win} u_i(t) + F_{win} w_{win}(t), \\ y_{win}(t) = C_{win} x_{win}(t), \end{cases} \tag{5}$$

where $x_{win}(t) = [x_i(t), \Delta P_{WTGi}]^\top$ and $w_{win}(t) = [w_i(t), \Delta P_{w-i}]$.

The wind power in (5) is established by P_{WTGi} and P_{w-i}. The output power change of WTG P_{WTGi} is added to the power system state vector. Wind power is considered a kind of energy injected into the power system. However, the relationship between wind speed and wind power output cannot be explained. In other words, the fluctuation of renewable energy is ignored.

(2) Uncontrollable weather conditions usually lead to variable of WTG output power. Therefore, the wind power model should fully consider the impact of external interference. To realize the control of output power from the WTG, the pitch control technique has been developed [10–12,21]. Using the output feedback signal of the WTG, the angle of the blades can be controlled, meaning that the optimum angle of the blades tracks the variation in wind speed.

Figure 3 provides the mathematical model of a Nordex N43 turbine [10–12,21], where ΔP_{GW} is the wind power output deviation, K_{p1}, K_{p2}, and K_{p3} represent the pitch control gain, hydraulic pitch actuator gain, and data fit pitch response gain, respectively, T_{p1}, T_{p2}, and T_{p3} make up the time constant, K_{pc} represents the blade characteristics, and K_{fc} is the fluid coupling gain. The control signal C_{1w} is obtained by the change in wind turbine mechanical output power. The inner controller C_{2w} is provided by C_{1w} and the inner process output $U_{1w}(s)$.

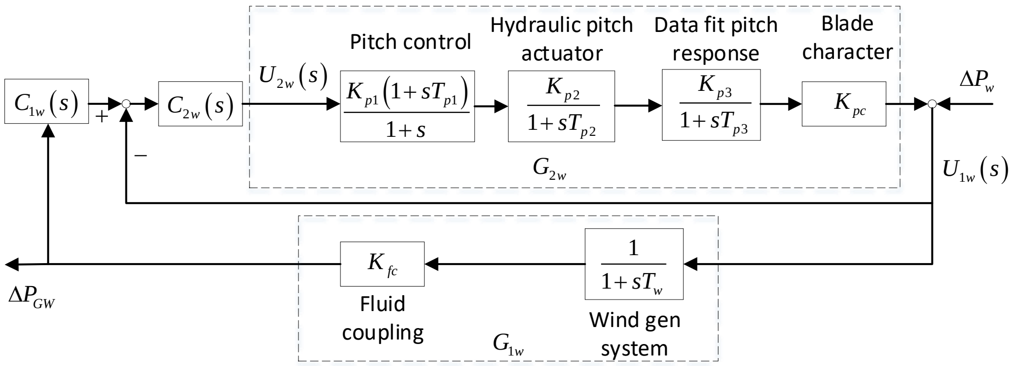

Figure 3. Mathematical relationships of a wind turbine generator.

The relationship between the active power and input wind speed can be presented as

$$P_{GW} = \frac{\rho a^2 V_w^3 C_p}{2}(T_{SR}, \beta) \tag{6}$$

where ρ (kg/m^3) and a (m^2) is the area density and swept, respectively. V_w (m/s) represents the wind speed, β (deg) represents the angle of the blade, T_{SR} represents the tip speed ratio, and the rotor efficiency C_p is provided as follows:

$$\begin{aligned} C_p &= \frac{T_{SR} - 0.022\beta^2 - 5.6}{2} e^{-0.17T_{SR}} \\ T_{SR} &= \frac{r_{pm}\pi D}{60V} \end{aligned} \tag{7}$$

where the rotor speed is r_{pm} and the diameter of blade rotor diameter is D (m). It is worth noting that, as wind power is a renewable energy source, the power supply is always determined by environmental factors.

Considering the signal transmission shown in Figure 3, the transfer functions G_{1w} and G_{2w} [10–12,21] are obtained for the wind farm system:

$$\begin{aligned} G_P(s) &= \frac{K_{p1}(1 + sT_{p1})}{(1 + s)}, G_H(s) = \frac{K_{p2}}{(1 + sT_{p2})}, \\ G_D(s) &= \frac{K_{p2}}{(1 + sT_{p2})}, G_I(s) = \frac{1}{(1 + sT_w)}. \end{aligned} \tag{8}$$

where pitch control is defined as G_P, the hydraulic pitch actuator is defined as G_H, the data fit pitch response is defined as G_D, and the induction generator is defined as G_I.

By constructing the mathematical relationship of the wind and the generator, the output wind power P_{WG} can be determined. The environment is considered based on the area density, swept area wind speed, and other factors. Differently, a few researchers have focused on the changes in the current and voltage of the WTG. According to the relationship between current and voltage, the WTGoutput can be easily obtained.

(3) Except for the turbine model in [10–12], a wind power generator can be modeled by considering changes in current and voltage [13,14,22,39–43]. In the wind power generation system, there exist different kinds of wind power generators, leading to different models.

A kind of squirrel-cage induction generator (SCIG) [14,22,39] has been widely considered for the output wind power. The SCIG is applied in wind power systems due to its high reliability and simple structure.

Figure 4 shows the basic configuration of the SCIG; P_g is defined as the output power of SCIG, which can be calculated by the voltage. The detailed mathematical relationship is as follows:

$$P_g = \frac{-3V^2 s(1+s)R_2}{(R_2 - sR_1)^2 + s^2(X_1 + X_2)^2} \tag{9}$$

where the synchronous angular speed is ω_0 , $s = \frac{\omega_0 - \omega}{\omega_0}$ is defined as the slip of generator, the stator resistance and reactance are defined as R_1 and X_1, respectively, and the rotor resistance and reactance are defined as R_2 and X_2, respectively. The wind power from SCIG is modeled for a multi-area power system in the case of $\omega \geq \omega_0$.

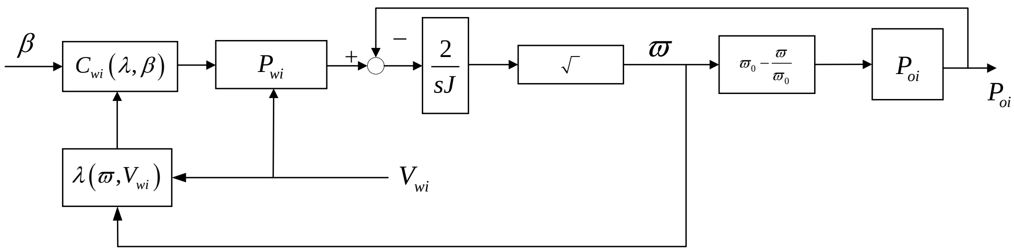

Figure 4. Mathematical relationship for SCIG.

In wind power systems, the electric power is produced by the wind turbine, which is driven by wind power. The power coefficient is defined as $C_p\{\lambda, \beta\}$, the pitch angle as β, and the area density as ρ, while A_i is the cross-section of the rotor. With these, the output power can be determined. Based on [14,22,39], the output power is defined as

$$P_w = \frac{C_p(\lambda, \beta) V_w^3 \rho A_i}{2} \tag{10}$$

where V_w is the wind speed. The mathematical relationship among the radius of the wind turbine R, the angular speed of the rotor ω, and the wind speed V_w is defined as the tip speed ratio $\lambda = \frac{R\omega}{V_w}$.

The following equation is used to obtain the angular speed of the rotor:

$$\omega^2 = \int \frac{2}{J}(P_w - P_g)dt \tag{11}$$

where the moment of inertia is defined as J. The pitch control system and hydraulic servo system have been studied based on the above definition. Compared with the explanation of a wind power system in [10–12,21], the relationship between the wind turbine and wind power is discussed in [14,22,39]. By constructing an SCIG mathematical model, it is possible to obtain find more information on the relationship between the turbine radius and the wind speed.

Another popular WTG for the wind power system is called a doubly-fed induction generator (DFIG). In [13,40–43], a DFIG system was discussed as a renewable resource. In previous survey research, it has been mentioned that most LFC wind power systems integrated with DFIG are trustworthy. To illustrate the difference between DFIG and [14,22,39,44,45], the mathematical structure of a simplified DFIG WTG is shown in Figure 5.

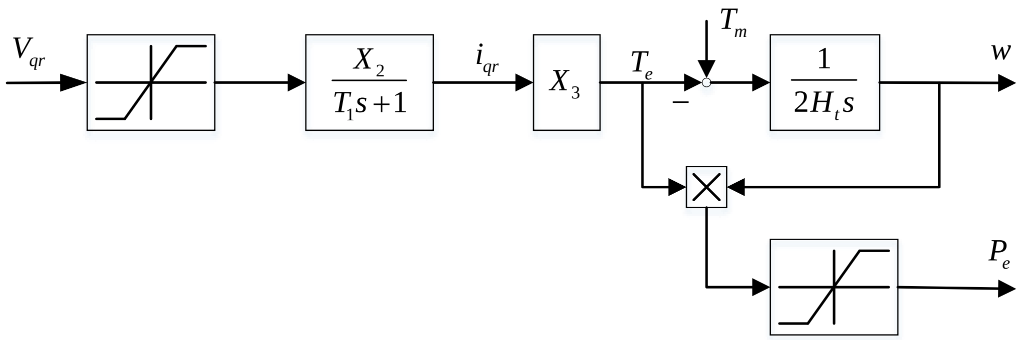

Figure 5. Mathematical relationships of DFIG.

Based on the above mathematical relationships, we have the following equation for the rotor current of the q-axis component:

$$\dot{i}_{qr}(t) = -\frac{i_{qr}(t)}{T_1} + \frac{X_2 V_{qr}(t)}{T_1}, \tag{12}$$

where $T_1 = \frac{L_0}{w_s R_1}$, $L_0 = L_r + L_m + \frac{L_m^2}{L_s + L_m}$, and $X_2 = \frac{1}{R_2}$, in which the magnetizing inductance is L_m, the rotor leakage inductance is L_r, the synchronous speed is w_s, and L_s represents the stator leakage inductance.

The rotational speed can be described by

$$\dot{w}(t) = -\frac{X_3 i_{qr}(t)}{2H_t} + \frac{T_m(t)}{2H_t}, \tag{13}$$

where H_t is the given constant, T_m represents the mechanical power, and $X_3 = \frac{L_m}{L_s + L_m}$.

Therefore, the active power of WTG is obtained as follows:

$$P_e(t) = w(t) X_3 i_{qr}(t), \tag{14}$$

The active power can be rewritten as

$$P_e(t) = w_p X_3 i_{qr}(t), \tag{15}$$

where w_p is the rotational speed at the operating point and the electromagnetic torque is described by

$$T_e(t) = i_{qs}(t) = -\frac{L_m}{L_s + L_m} i_{qr}(t). \tag{16}$$

Defining $x_w(t) = [\Delta X_{gi}(t), \Delta P_{gi}(t), \Delta f_i, \Delta P_{tie}^i(t), \Delta i_{qr,i}(t), \Delta w_i(t), \Delta E_i(t)]^\top$, the WTG power system state equation is obtained as follows:

$$\dot{x}_w(t) = A_w x_w(t) + B_w u_w(t) + F_w \Delta P_{di}(t). \tag{17}$$

In this subsection, we have discussed the different models of wind power. First, we introduced wind power as directly considered in the power system, with renewable resource energy supported by a capacity wind induction generator. Then, we discussed how to control the WTG through the pitch control method. Lastly, we considered how the different kinds of wind power generators influence the construction of power system models integrated with WTG. As a result of differences in the internal structure of various generators, their mathematical models are different. Focusing on this, the working principles of the SCIG WTG and DFIG WTG are described in detail using mathematical relationships.

3.1.2. Solar Energy

Another important and common renewable energy source is solar energy. To capture solar energy and make full use of it, a proper device must be used. There are two main methods of using solar energy [21].

(1) A large diode PV panel is subjected to sunshine. Using PV panels, solar energy is converted into a current that can be transmitted through conducting wires. In theory [46], an ideal PV solar energy can be modeled as the integration of a photocurrent source and diode. The variation in ambient temperature and sunlight irradiance is proven to influence the power supplied by PV panels [12]. To study the solar energy applied in power systems, a simplified PV panel model can be constructed considering the relationship of various electronic components [12,21,33].

The single-diode PV module equivalent circuit model is shown in Figure 6.

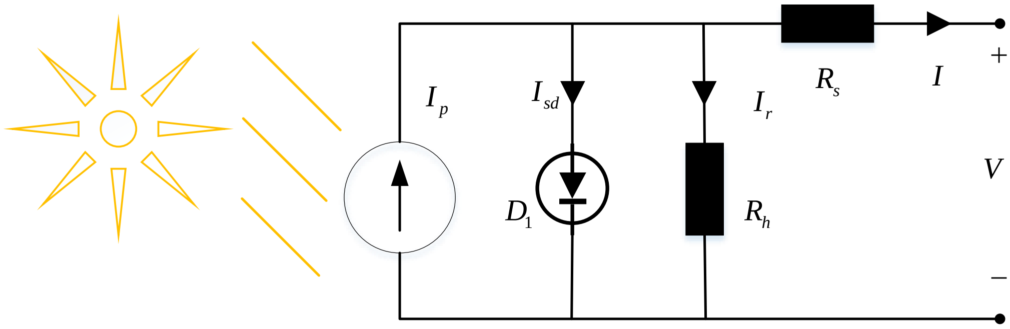

Figure 6. Simplified model of single-diode PV.

To analyze the voltage and current of the PV panel, the photocurrent I_P is considered. The PV current is described by the following equation:

$$I = I_p - I_{sd} - I_r \tag{18}$$

where I_p, I_{sd}, and I_r are the photocurrent, diode current, and current of the parallel resistance, respectively.

When subjected to sunshine at a certain temperature, a PV produces a photocurrent I_p, which can be described as follows:

$$I_p = I_S(\frac{S}{1000}) + J_t(T - T_{re}) \tag{19}$$

where S represents the solar irradiance, I_s represents the short-circuit current, J_t represents the temperature coefficient, T represents the PV temperature, and T_{re} represents the reference temperature.

The diode current I_{sd} can be expressed as

$$I_{sd} = I_o\left[\exp(\frac{V + IR_s}{nmT}) - 1\right] \tag{20}$$

in which the terminal voltage V, current I, series resistance R_s, diode ideality factor n, and Boltzmann's constant m are considered. The saturation current I_o can be obtained by

$$I_o = I_d(\frac{T}{T_{re}})^3\exp\left[\frac{qE_g}{nm}(\frac{T - T_{re}}{T_{re}T})\right] \tag{21}$$

where I_d is the diode reverse current, E_g is the bandgap energy of the cell semiconductor, and q is the charge of the electron.

Finally, I_r can be obtained as follows:

$$I_r = \frac{V + IR_s}{R_h} \tag{22}$$

where R_h is the parallel resistance.

In several studies [16,21,47,48], a first-order transfer function has been constructed to described the PV system. The transfer function of the PV–grid interface is

$$\Delta P_v = \frac{K_{pv}}{1 + sT_{pv}} \Delta P_{solar} \tag{23}$$

where K_{pv} is the gain of the PV and can be chosen as one, while T_{pv} is the time constant. The dynamic behavior of the PV power conversion systems is neglected.

It is worth noting that a double-diode PV model can be designed by using two diodes [33]. A model with diodes D1 and D2 is shown in Figure 7. The mathematical relationships of a two-diode PV system are mostly the same as in one-diode PV systems.

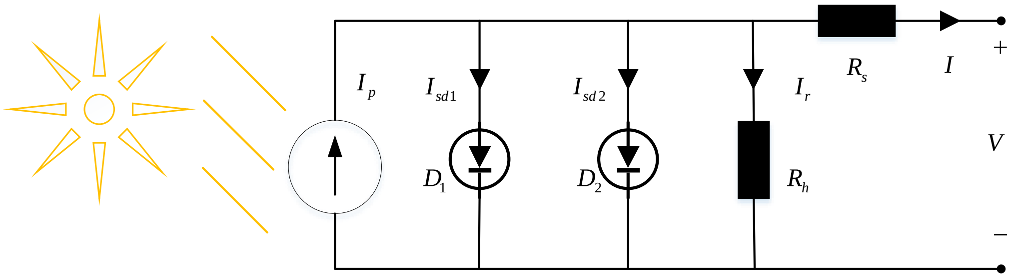

Figure 7. Simplified circuit model of two diode PV module.

(2) Solar thermal technologies are another technique to extract power from sunshine. Solar energy is transferred to a thermodynamic cycle to drive a mechanical device, creating electricity. It is worth noting that more governors and turbines are used in the solar thermal power system. Unlike wind power plants and PV power plants, an autonomous controller is needed for LFC solar thermal power systems [21]. The solar thermal power system model can be described using the solar energy, control signal, governor, and turbine, as shown in Figure 8.

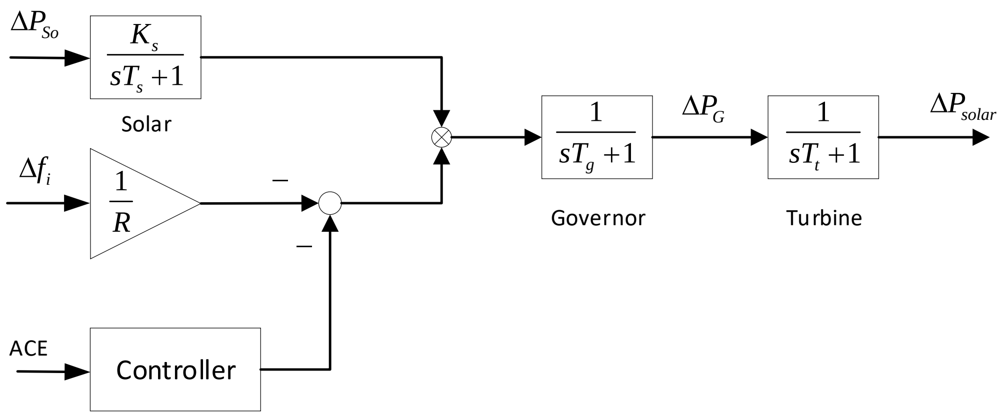

Figure 8. Simplified circuit model of a solar thermal power system.

Similarly, solar thermal technology can be represented as a first-order lag [49]. Based on signal transmission, we have

$$\Delta P_{solar} = \frac{1}{sT_t + 1} \Delta P_G \tag{24}$$

where K_S is the solar energy gain, T_s is the time constat of collar energy, and T_g and T_t are the time constant of governor and turbine, respectively. The ACE signal is taken as the control input in the LFC strategy. Figure 8 shows the steam produced in the heat exchangers to drive the turbine. Further, the deviation of ΔP_{solar} is considered in the power system and influences the balance of load and frequency.

Uncertainty or disturbance due to renewable energy sources cannot be avoided. The intermittent nature of renewable energy sources, system uncertainties with respect to the control and parameters, and linearization error all increase the difficulty of the LFC problem. Furthermore, there exist parameter uncertainties in any practical power system due to the changes and constantly varying load at the operation point. An uncertainty model with bounded uncertainties [50,51] can be defined as follows:

$$g_i(t) = \Delta A_i x_i(t) + \Delta B_i u_i(t) + (F_i + \Delta F_i)(\Delta P_{di} + P_{gi}) \quad (25)$$

where ΔA_i, ΔB_i, ΔF_i are mismatched parametric uncertainties, ΔP_{di} is the system disturbance, and P_{gi} represents the uncertainty in the renewable energy source.

It can be understood that renewable energy is important to our life and industry. Reasonable and efficient use of these energy sources can undoubtedly reduce the pressures caused by obtaining electric power in traditional ways. To estimate the disturbance due to load demand, system uncertainty, and WTG, in [52] the authors proposed an extended state observer. In another study, an LFC method was applied to ensure the performance of multi-area wind power systems [53]. Generally, wind power fluctuation, load disturbances, and system parameter uncertainties lead to larger voltage deviation [54]. Due to the complexity of the actual situation, different modeling methods can provide different solutions for the efficient use of renewable energy. Model description can help to handle the LFC issues in today's modern power systems, and as such is an important research area closely connected with renewable energy.

3.2. Electric Vehicles

To achieve low-carbon targets, EVs represent an excellent advance. EVs can help to improve the power grid's load factor while minimizing fluctuations. In addition, the integration of electric vehicles into the power system can balance power demand and reduce the prime cost of electricity supply [55]. Positive externalities for renewable energy integration from the side of power supply can be served by EVs [23]. The ratio of coverage of EVs helps to determine the power system's operation. This means that reasonable use of EVs offers a chance to accelerate the transformation of the power system.

In EVs, the battery is the unique power supply. The battery has to face the problems of reliability, safety, and lifetime, which are key factors in realizing widespread coverage of EVs. The battery's state of charge (SOC) reveals the relationship between stored energy and its capacity, which is an important feature of an EV. Considering an electric vehicle connected to the power system, a simplified model is shown in Figure 9.

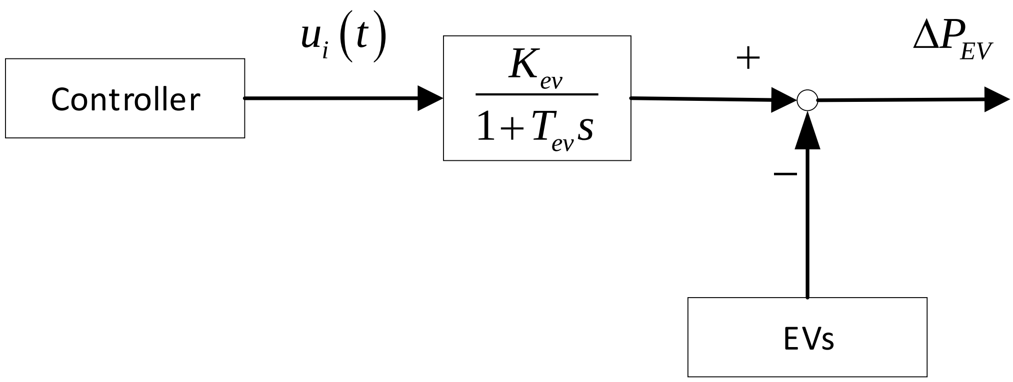

Figure 9. Simplified model of electric vehicle for LFC.

The power output deviation of the EVs can be described as

$$\Delta \dot{P}_{EV} = \frac{K_{ev}}{T_{ev}} u_i(t) - \frac{1}{T_{ev}} \Delta P_{EV} \tag{26}$$

where K_{ev} is the EV gains and T_{ev} represents the constant parameters. Defining $\hat{x}_i(t) = [x_i(t), \Delta P_{EV}]$, a power system model with EVs can be constructed easily. To clearly analyze the LFC problem, we need to know the inner signal transmission.

Furthermore, it is necessary to explore the EV model in a way that can explain the impact of EVs on the LFC. A straightforward EV model is proposed in Figure 10.

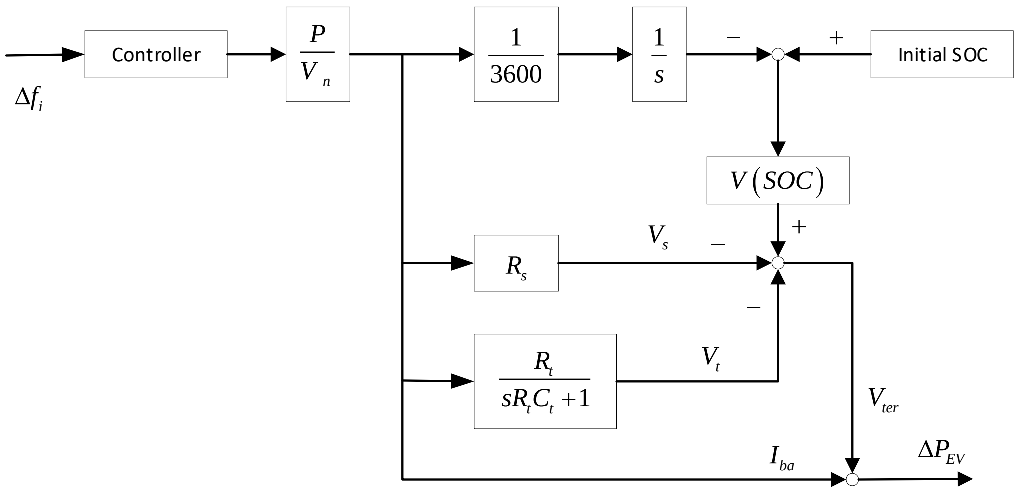

Figure 10. Dynamic model of EV for LFC.

The electric vehicle model consists of an open circuit voltage source connected in series, with a series resistance Rs and a parallel branch R_t, C_t [56]. The terminal electric vehicle voltage can be obtained according to the the open-circuit voltage and the voltage drop across the series resistance and the R, C branch. Based on the mathematical relationship in Figure 10, the relationship between the electric vehicle open circuit voltage $V(SOC)$ and nominal voltage V_n is as follows:

$$V(SOC) = V_n + \frac{SRT}{F} ln(\frac{SOC}{C_n - SOC}) \tag{27}$$

where F, T, R, are constant parameters and S is the sensitivity parameter between SOC and open circuit voltage.

Integration of power systems with EVs has become a primary research area, with a particular focus on EVs and power system operation. Optimized charging for reduced cost, electricity market participation, and scheduling and control techniques are among the most considered directions. Importantly, it is necessary to avoid causing network overloading or compromising system stability due to EV charging.

3.3. Cyber-Attacks

The timescale of seconds on which LFC signals are generated means that complex data validation algorithms cannot be used for estimation and validation of measurement data. This has contributed to issue of attackers being able to rewrite transmitted data by exploiting simple mathematics [57]. This is a major reason for power systems being easily damaged by cyber-attacks. Weaknesses or characteristics that exist in the power system can be used by attackers to design possible attack strategies. It is possible to mitigate or eliminate the impact of attacks on the power system by designing detection or control methods. To construct data integrity attacks, a common assumption about attackers having prior model knowledge of physical systems was relaxed in [58]. In the view of [24], DoS attacks and data integrity attacks are the most common cyber-attacks targeting LFC signals.

Normally, it is necessary to assume a particular attack type. Therefore, we focus here on the impact of the most typical DoS and deception attacks.

3.3.1. Dos Attacks

When a DoS attack occurs, communication resources become occupied and transmission signals are delayed, causing devices to operate under incorrect conditions. DoS attacks take two forms, namely, stochastic and queueing.

(1) A Bernoulli process or Markov process is used to build a DoS attacks model. In such models, there is a possibility of a DoS attack happening in the communication channel at each sampling moment.

A power system model under DoS attack with a Bernoulli process [25,26,59] is provided as follows:

$$\begin{cases} \dot{x}_i(t) = A_i x_i(t) + (1-\alpha_i)B_i u_i(t_k) + \alpha_i B_i u_i(t_{k-1}) + F_i w_i(t), \\ y_i(t) = C_i x_i(t), \end{cases} \tag{28}$$

in which $\alpha_i \in 0,1$ is the Bernoulli distribution related to occurrences of DoS attack, and is described as

$$E(\alpha_i) = \alpha, E((\alpha_i - \alpha)^2) = \alpha(1-\alpha), \tag{29}$$

where α is the probability of a DoS attack.

A power system model under DoS attack with a Markov process [60] can be described as follows:

$$\begin{cases} \dot{x}_i(t) = A_i x_i(t) + \beta_i B_i u_i(t) + F_i w_i(t), \\ y_i(t) = C_i x_i(t), \end{cases} \tag{30}$$

where $\beta_i \in \{0,1\}$ represents the Markov modulated attack sequence that prevents the signal from being transmitted to the next device.

(2) In the queueing model, the DoS on/off action h_n is considered, assuming the time instants at which the action of DoS on/off is changed (when it is possible to interrupt communication). The following time interval describes the sequence of DoS attacks:

$$H_n = h_n \cup [h_n, h_n + \tau_n] \tag{31}$$

where τ_n is the attack length during which communication is interrupted. When $\tau_n = 0$, a single pulse at time h_n can be seen as the sequence of DoS attacks. The most recent data received from the controller during the DoS attack are taken as the actuator signal, while $\Gamma(t)$ is the time interval.

$$\Gamma(t) = [\tau, t] \setminus \{H_n \cap [\tau, t]\} \tag{32}$$

3.3.2. Deception Attacks

False data injection (FDI) attacks and malicious attacks, and are defined as deception attacks on the LFC. Deception attacks seek to modify the transmitted information at certain points in an LFC power system [61]. Due to the different possible attack modes, there are many types of deception attacks.

First, we consider deception attacks to inject false data into the power system. These deception attacks corrupt the real-time transmission signal in the LFC power system. To realize this, deception attacks target the control or measurement channels. The attack vectors are designed based on attack templates or data corruption strategies. The state space function under deception attack is as follows:

$$\begin{cases} \dot{x}_i(t) = A_i x_i(t) + B_i(u_i(t) + \alpha_i D_{F1}) + F_i w_i(t), \\ y_i(t) = C_i x_i(t) + \alpha_i D_{F2}, \end{cases} \tag{33}$$

in which α_i is the Bernoulli distribution related to occurrences of deception attacks, D_{F1} are the deception attacks on the actuator, and D_{F2} are deception attacks on the system output.

In addition, deception attacks can be implemented by replaying recorded data. This kind of deception attack is called a replay attack. First, a disclosure attack is carried out to gather data sequences from the compromised resources. Then, the gathered data sequences are replayed. Replay attacks exploit valid data via delayed transmission or repeat the same signal fraudulently [62]. For example, attackers may iterate past data from the attacked actuators or sensors for a definite time in a Byzantine replay attack. A sensor channel under replay attack can be described as follows:

$$D_a = -Cx_i(t) + y_i(t - \tau_i(t)) \tag{34}$$

where $\tau_i(t) \in (0, t)$, $y_i(t - \tau)$ represents the sensor data. Replay attacks can be described as time-varying delays $\tau_i(t)$, in which the rate of change and upper bound are unknown. Replay attacks have the characteristic of a distinct monitoring phase and replay phase.

In addition to the types of deception attacks mentioned above, other deception attacks may involve covert attacks [58], zero-dynamics attacks [63], and more.

4. Strategies

In this section, we describe the various control strategies, including classical control, modern control, and intelligent control. New challenges such as renewable energy, electric vehicles, and cyber-attacks raise the degree of difficulty; therefore, modern control methods have been developed and applied to guarantee stable systems [64]. With the continuous development of artificial intelligence [28], many excellent new data-driven control methods have been applied to solving LFC problems.

4.1. Classical Control Method

Of the classical control methods, the most considered are PI and PID. In LFC, PI or PID control methods use the tie-line power deviation and frequency deviation to design the controller. As shown in Figure 2, the area control error ACE_i is summarised based on the signal transmission ΔP_{tie} and Δf_i. The PI controller is given as

$$u_i = K_p ACE_i + K_i \int ACE_i \tag{35}$$

where K_p, K_i represent the controller gain. By defining $y_i(t) = [ACE_i, \int ACE_i]$, the controller can be expressed as

$$u_i = K_{pi} y_i(t) \tag{36}$$

where $K_{pi} = [K_p, K_i]$, K_{pi} will be designed.

The PID controller [19,65,66] can be designed as follows:

$$K_i(s) = K_p + \frac{K_i}{s} + sK_d \tag{37}$$

and the control input is

$$u_i = K_i(s) y_i(t) \tag{38}$$

Based on the frequency-domain approach, a fractional order PID controller cascaded with a first-order filter for the delayed LFC system was discussed in [67]. By using an improved version of particle swarm optimization [16], a PID-based secondary controller was proposed to stabilize the system. Based on the gain-scheduling decentralized (GSD) scheme, the authors in [68] compared a GSD-PID controller and a GSD-PI controller. To overcome uncertainties and reduce the computational cost, the authors of [69] described a novel numerical method to obtain stabilizing sets of PID or PI controllers. A tuning-free PID control strategy was developed in [70].

To address recent challenges, PI and PID controllers for LFC power systems have been widely researched. In [71], a hybridized fuzzy-PI-linear active disturbance rejection controller was designed for a power system with renewable energy and EVs. In [27], the $H-\infty$ performance was guaranteed by an event-based PI LFC scheme for power systems suffering from deception attacks. In [72], a novel cascade fractional order controller comprising a three-degrees-of-freedom PID and tilt-integral controllers was proposed for dealing with the LFC issue in a WTG power system. A PID controller was applied as the supplementary control task in a renewable power system in [20]. A PID and fuzzy controller were integrated into a fractional order environment for stabilizing power system frequency in [73].

4.2. Modern Control Method

Many control strategies have been developed for the LFC issue, including adaptive control, variable structure, intelligent techniques, digital control, and robust control. In variable structure control methods, SMC is a typical example. Aside from its simple implementation, SMC is insensitive to disturbance and parameter variations [74]. It is important that the useable sliding mode surface satisfies $s(t)=0$ and $\dot{s}(t)=0$. Researchers have made many attempts to design a proper SMC.

In [13,75,76], a kind of PI-type SMC was applied to an LFC power system

$$s(t)=G_i x_i(t)-\int_0^t G_i(A_i-B_iK_i) \tag{39}$$

where G_i and K_i are a constant matrix and G_i is chosen to ensure that G_iB_i is non-singular.

Mostly, the system state is applied to the SMC design. However, in many cases only the system output is available, such as in the case of system states that cannot be completely measured or may be overly costly to measure. Therefore, two kinds of methods are provided to design the output sliding mode controller [77]; the first is to estimate the states of the system using a state observer, while the second is to design the controller using the system output directly. Based on the system state and output, an output sliding mode surface [78] is designed as

$$s(t)=G_i y_i(t)-\int_0^t C_i x_i(\vartheta)d\vartheta \tag{40}$$

where $y_i(t)$ is the system output and G_i is selected to ensure that $G_iC_iB_i$ is non-singular. The problems of system states that cannot be completely used are well solved by the output feedback SMC. In addition, considering the uncertainty or disturbance that exists in renewable power systems, a full-order observer can be applied to estimate the states of the system [79]. An output-dependant SMC was designed as follows:

$$s(t)=G_i(y_i(t)-y_i(0))-\int_0^t L_i(q)dq \tag{41}$$

with observed data $L_i(t)$ as follows:

$$L_i(t)=-K_i(x_i(t)-e_i(t)) \tag{42}$$

where $e_i(t)$ is the state error.

On this basis, many excellent designs of sliding mode surfaces have been proposed. An adaptive fast terminal sliding mode controller was designed in [80] in which the bound of the unknown disturbances was estimated using an adaptive law. The authors of [52] designed a fractional-order integral SMC that avoided chattering of the frequency deviation. The authors of [53] explored the design of a derivative and integral terminal SMC strategy to handle the LFC problem. By taking advantage of the adaptive SMC and sliding mode observer, a novel control strategy can be proposed to help stabilize power systems [54]. Most control problems are solved by the design of the controller, and as such the controller needs to be seen as completely believable. However, many neglected factors, such as the round-off error in numerical computation, the aging/failure of system components, and the finite precision of measuring equipment can make the related assumptions may be infeasible [81].

To theoretically guarantee system stability, the controller should be designed to suppress the entire uncertainty. In subsection 3.1, we show how uncertainties or disturbances from renewable energy can be considered together using an aggregated mismatched uncertainty $g_i(t)$ model. Similarly, it is possible that there may exist uncertainty in the controller. To describe such situations, the non-fragile control problem is proposed. A non-fragile controller is described as

$$\tilde{K}_i = K_i + \Delta K_i \tag{43}$$

where the controller gain perturbation ΔK_i is defined as

$$\Delta K_i = M_i \xi_i N_i \tag{44}$$

with the uncertainty matrix satisfying $\|\xi_i\| < I$, M_i, and N_i being the constant matrix.

To obtain a more practical controller, the non-fragile control problem can be used. In [81], an extended dissipative fuzzy non-fragile PID controller was designed with controller parameter perturbations. The authors in [82] proposed a non-fragile control approach such that the controller parameter variations can be ignored without loss of system performance. Considering the existence of control uncertainty, a non-fragile PI-control scheme [34] was discussed in the context of the LFC approach for nonlinear power systems. For a linear control system under DoS attack, a non-fragile feedback controller was applied in [83]. Considering uncertainties and external disturbances EVs power system, a full-order observer-based finite-time non-fragile LFC was designed in [84].

4.3. Intelligent Control

Intelligent control can be applied to improve the performance of LFC power systems. With intelligent control, relevant information about the power system is processed based on algorithms or logic. With the increasing size scale of power systems and data, it may be doubted whether data-driven control schemes represent a promising solution to balancing system frequency. In [85], a fuzzy-PSO-PIDLFC was obtained based on particle swarm optimization (PSO). Based on multi-agent deep reinforcement learning with continuous action domain, a data-driven cooperative LFC method for a power system was discussed in [37]. To realize the LFC strategy, area control errors need to be minimized. The objective Q is defined as unscheduled tie-line power flow interchange and the squared sum of frequency deviations [37], which is provided as

$$Q^{\mu}(s, \alpha) = -\sum_{t=1}^{T} [\Delta t \sum_{i=1}^{n} [(\beta_i \Delta f_i)^2 + (\Delta P_{tie})^2]] \tag{45}$$

where s is the state information, Δt is the step size, and T represents the simulated total time. After exploration, the system frequency under the data-driven strategy is suitable for all scenarios. During centralized learning, a multi-agent deep deterministic policy gradient is applied to determine the controller parameters, which is optimized based on the coordinates in order to improve the load frequency control performance. An agent parameters initialization process is applied to accelerate the process of multi-agent deep reinforcement learning.

In addition, the data-driven method can be applied to improve the performance of traditional or modern control methods [86,87]. This means that data-driven control has great development potential in control theory. Many strategies have been proposed to realize data-driven LFC. An improved version of particle swarm optimization was developed to accelerate the optimization of the nonlinear LFC problem in [68]. Based on hybrid bacteria foraging-oriented particle swarm optimization, a linear quadratic regulator (LQR) controller was designed for AGC in [88]. PSO was applied to help design a fractional-order type-2 fuzzy logic controller for a frequency control problem of a renewable power system in [38]. To realize LFC, a generalized compression neural network (GRNN) was integrated for the design of a controller in [89]. In [71], optimal controller parameters were obtained using a new quasi-opposition-based artificial electric field algorithm. The selection of controller parameters is always a major challenge; the imperialist competitive algorithm was fruitfully exploited for solving this problem in [90]. Based on deep reinforcement learning in the continuous action domain, a model-free method for data-driven LFC was developed for renewable power systems with uncertainties in [91]. In [92], an event-triggered data-driven model-free adaptive LFC method was proposed for power systems. To solve the randomness from the power load demand and renewable generations, an adaptive learning strategy was applied in [93] to design the SMC for an LFC power system. An evolutionary imitation curriculum multi-agent deep deterministic policy gradient algorithm was developed in [28] to realize coordinated control.

4.4. Others

In addition to the control methods mentioned above, there are many control methods with excellent performance in solving LFC problems. In [94], the authors attempted to realize the integration of renewables into modern power systems using the concept of a grid-forming (GFM) converter. A whale optimization algorithm was used in [95] to enhance the virtual inertia control loop by optimizing the parameters of a virtual inertia controller while considering the uncertainties of system inertia with renewable energy sources. Virtual inertia control was applied to the parameter regulator of a WTG based on direct heuristic dynamic programming in [96]. In [97], a new application of a robust virtual inertia control-based coefficient diagram method controller was proposed for an islanded MG considering high-level RES penetration for enhancement of system validity and robustness in the face of disturbances and parametric uncertainties. In [98], dynamic deloading was proposed considering the influence of the safe limit of a WTG, the wind power prediction error, spinning reserve of the SG, and system operating costs. Based on a deep learning algorithm, an adaptive nonlinear deloading strategy for a wind turbine generator integrated with an interconnected LFC power system was proposed in [99]. The salp swarm algorithm (SSA) ws applied to promote the LFC performance of a multi-area hybrid renewable nonlinear power system in [100]. An optimal LFC was designed through combined state and control gain estimation for noisy measurements in [101]. A decentralized resilient $H-\infty$ LFC was proposed in [102] for multi-area power systems under DoS attacks.

5. Conclusions and Future Directions

5.1. Conclusions

This survey has explored the recent challenges in LFC power systems. Focusing on the mathematical modeling and state space function, the effect of certain challenges (wind, solar, EVs, and cyber-attacks) facing power systems has been investigated in detail. For all of these different challenges, we have considered the problem from the perspective of the relevant models and power system state function. For each challenge, we have analyzed the impact on the power system from the perspective of different models. This survey has shown that identifying the most common types of cyber-attacks targeting the LFC helps in formulating reasonable and effective control strategies. Aiming at the uncertainty problems that many researchers ignore, this paper studies renewable energy uncertainty and controller uncertainty. To handle such challenges in the LFC power systems, different control methodologies have been studied for traditional control, modern control, and intelligent control. According to publications on recent challenges and control methods, the deficiencies of existing research have been identified, which can help to inspire future researchers to seek more reliable and efficient control methods.

5.2. Future Directions

At present, the stability problem and communication security problem with respect to renewable energy interconnected power systems is well worth noting. Integration and optimization of multiple renewable energy sources represents a major challenge facing future research. Furthermore, the development of innovative technologies such as cloud computing, big data, and artificial intelligence shows great potential for solving LFC-related problems. The current challenges and future research directions are discussed below.

(1) Renewable energy. With the deepening of research on renewable energy, certain sources of renewable energy that could not be used before have been gradually developed for power systems. The diverse power output of renewable energy sources connected to the power system increases the complexity variability in terms of power generation and adds uncertainty. This presents challenges for the stabilization of LFC power systems integrated with renewable energy sources. In addition, the integration of multiple renewable energy sources means that more electronic equipment needs to be used. The resulting need to ensure matching between devices, efficient information transmission, and other issues are unavoidable challenges facing LFC power systems.
(2) Cyber security. Cyber-security problems are directly related to the normal operation of power systems. Compared with a single type of cyber-attack, hybrid cyber-attacks can have greater impact. Furthermore, new types of cyber-attacks on LFC power systems deserve attention. According to our investigation, most of the cyber-attacks considered in the context of LFC power systems can be modeled using the queueing model or stochastic model. However, the types of cyber-attack are increasing. One possible development direction of cyber-attacks involves smart design. For example, attackers may use devices to obtain information about the power system and determine vulnerable nodes in the network according to the obtained information. Cyber-attacks are expected to remain an important problem in LFC power systems in the future.
(3) Control capability. In recent years, a large number of intelligent algorithm-based control methods have been researched for LFC power systems. Multiple issues around renewable energy, cyber-attacks, and other issues are focusing greater development space and attention on intelligent control methods. How to improve control capability is becoming an important issue. To achieve this goal, researchers need to choose their research direction; possibilities include combining traditional control methods with modern control methods, using intelligent control methods, and developing new intelligent algorithms.
(4) Flexibility. A highly flexible and secure interconnected power system is a necessity due to the high penetration and networking requirements of renewable energy sources. The transition of the current energy production mix can be aided by hosting a larger proportion of renewable energy sources. In this way, multi-area power system can become more flexible and reliable, resulting in the development of novel intelligent algorithms along with control, storage, and market approaches.

Author Contributions: Conceptualization, X.L. and S.Q.; methodology, S.Q.; validation, X.L., S.Q. and Z.L.; formal analysis, X.L.; investigation, S.Q.; resources, Z.L.; data curation, S.Q.; writing-original draft preparation, S.Q.; writing-review and editing, X.L. and Z.L.; visualization, S.Q.; supervision, X.L.; project administration, Z.L.; funding acquisition, X.L. All authors have read and agreed to the published version of the manuscript.

Funding: This work was supported in part by the National Natural Science Foundation of China under Grant U2003110, 61973133, and in part by and the Natural Science Foundation of Hubei Province of China under the Grant No. 2022CFA052, and in part by the Key Laboratory Project of Shaanxi Provincial Department of Education (No. 20JS110), and in part by the Thousand Talents Plan of Shaanxi Province for Young Professionals.

Institutional Review Board Statement: Not applicable.

Informed Consent Statement: Informed consent was obtained from all subjects involved in the study.

Data Availability Statement: Not applicable.

Conflicts of Interest: The authors declare that they have no known competing financial interest or personal relationships that could have appeared to influence the work reported in this paper.

References

1. Arya, Y.; Dahiya, P.; Celik, E.; Gulshan, C.; Gozde, H,; Nasiruddin, I. AGC performance amelioration in multi-area interconnected thermal and thermal-hydro-gas power systems using a novel controller. *Eng. Sci. Technol. Int. J.* **2021**, *24*, 384–396. [CrossRef]
2. Tao, T.; Roy, S.; Baldi, S. Stable adaptation in multi-area load frequency control under dynamically-changing topologies. *IEEE Trans. Power Syst.* **2020**, *36*, 2946–2956. [CrossRef]
3. Shangguan, X. C.; He, Y.; Zhang, C. K.; Yao, W.; Zhao, Y.; Jiang, L.; Wu, M. Resilient load frequency control of power systems to compensate random time delays and time-delay attacks. *IEEE Trans. Ind. Electron.* **2022**, *70*, 5115–5128. .. [CrossRef]
4. Yan, S.; Gu, Z.; Park, J. H.; Xie, X.; Dou, C. Probability-density-dependent load frequency control of power systems with random delays and cyber-attacks via circuital implementation. *IEEE Trans. Smart Grid* **2022**, *13*, 4837–4847. [CrossRef]
5. Zhang, G.; Li, J.; Bamisile, O.; Xing, Y.; Cai, D.; Huang, Q. An H_∞ load frequency control scheme for multi-area power system under cyber-attacks and time-varying delays. *IEEE Trans. Power Syst.* **2022**, *38*, 1336–1349. [CrossRef]
6. Yan, S.; Gu, Z.; Park, J. H. Memory-event-triggered H_∞ load frequency control of multi-area power systems with cyber-attacks and communication delays. *IEEE Trans. Netw. Sci. Eng.* **2021**, *8*, 1571–1583. [CrossRef]
7. Liu, X.; Bai, D.; Sun, B.; Wen, J.; Lv, W.; Li, K. Event-triggered sliding mode load frequency control for multi-area interconnected power systems under deception attacks. *J. Univ. Sci. Technol. China* **2021**, **51**, 33–42.
8. Shangguan, X. C.; He, Y.; Zhang, C. K.; Jiang, L.; Spencer, J. W.; Wu, M. Sampled-data based discrete and fast load frequency control for power systems with wind power. *Appl. Energy* **2020**, *259*, 114202. [CrossRef]
9. Wang, Z.; Liu, Y.; Yang, Z.; Yang, W. Load frequency control of multi-region interconnected power systems with wind power and electric vehicles based on sliding mode control. *Energies* **2021**, *14*, 2288. [CrossRef]
10. Hasanien, H. M. Whale optimisation algorithm for automatic generation control of interconnected modern power systems including renewable energy sources. *Iet Gener. Transm. Distrib.* **2018**, **12**, 607–614. [CrossRef]
11. Hasanien, H. M. A set-membership affine projection algorithm-based adaptive-controlled SMES units for wind farms output power smoothing. *IEEE Trans. Sustain. Energy* **2014**, *5*, 1226–1233. [CrossRef]
12. Abou El-Ela, A. A.; El-Sehiemy, R. A.; Shaheen, A. M.; Diab, A. E. G. Design of cascaded controller based on coyote optimizer for load frequency control in multi-area power systems with renewable sources. *Control Eng. Pract.* **2022**, *121*, 105058. [CrossRef]
13. Mani, P.; Joo, Y. H. Fuzzy logic-based integral sliding mode control of multi-area power systems integrated with wind farms. *Inf. Sci.* **2021**, *545*, 153–169. [CrossRef]
14. Mi, Y.; Hao, X.; Liu, Y.; Fu, Y.; Wang, C.; Wang, P.; Loh, P. C. Sliding mode load frequency control for multi-area time-delay power system with wind power integration. *IET Gener. Transm. Distrib.* **2017**, *11*, 4644–4653. [CrossRef]
15. Bakeer, A.; Magdy, G.; Chub, A.; Bevrani, H. A sophisticated modeling approach for photovoltaic systems in load frequency control. *Int. J. Electr. Power Energy Syst.* **2022**, *134*, 107330. [CrossRef]
16. Alayi, R.; Zishan, F.; Seyednouri, S. R.; Kumar, R.; Ahmadi, M. H.; Sharifpur, M. Optimal load frequency control of island microgrids via a PID controller in the presence of wind turbine and PV. *Sustainability* **2021**, *13*, 10728. [CrossRef]
17. Ahmed, M.; Magdy, G.; Khamies, M.; Kamel, S. Modified TID controller for load frequency control of a two-area interconnected diverse-unit power system. *Int. J. Electr. Power Energy Syst.* **2022**, *135*, 107528. [CrossRef]
18. Sharma, G.; Narayanan, K.; Adefarati, T.; Sharma, S. Frequency regularization of a linked wind-diesel system using dual structure fuzzy with ultra-capacitor. *Prot. Control Mod. Power Syst.* **2022**, *7*, 12. [CrossRef]
19. Fathy, A.; Alharbi, A. G. Recent approach based movable damped wave algorithm for designing fractional-order PID load frequency control installed in multi-interconnected plants with renewable energy. *IEEE Access* **2021**, *9*, 71072–71089. [CrossRef]
20. Vedik, B.; Kumar, R.; Deshmukh, R.; Verma, S,; Shiva, C. K. Renewable energy-based load frequency stabilization of interconnected power systems using quasi-oppositional dragonfly algorithm. *J. Control. Autom. Electr. Syst.* **2021**, *32*, 227–243. [CrossRef]
21. Sobhy, M. A.; Abdelaziz, A. Y.; Hasanien, H. M.; Ezzat, M. Marine predators algorithm for load frequency control of modern interconnected power systems including renewable energy sources and energy storage units. *Ain Shams Eng. J.* **2021**, *12*, 3843–3857. [CrossRef]
22. Uehara, A.; Senjyu, T.; Yona, A.; Funabashi, T. A frequency control method by wind farm and battery using load estimation in isolated power system. *Int. J. Emerg. Electr. Power Syst.* **2010**, *11*, 2. [CrossRef]
23. Wu, W.; Lin, B. Benefits of electric vehicles integrating into power grid. *Energy* **2021**, *224*, 120108. [CrossRef]
24. Mohan, A. M.; Meskin, N.; Mehrjerdi, H. A comprehensive review of the cyber-attacks and cyber-security on load frequency control of power systems. *Energies* **2020**, *13*, 3860. [CrossRef]
25. Hossain, M. M.; Peng, C.; Wang, Y. L.; Du, X. Handshake logic-based event-triggered load frequency control for smart grids under DoS attacks. *IEEE Trans. Ind. Inform.* **2021**, *18*, 3863–3872. [CrossRef]
26. Yang, J.; Zhong, Q.; Shi, K.; Zhong, S. Dynamic-memory event-triggered H_∞ load frequency control for reconstructed switched model of power systems under hybrid attacks. *IEEE Trans. Cybern.* **2022**, 1–13. [CrossRef] [PubMed]
27. Wang, D.; Chen, F.; Meng, B.; Hu, X.; Wang, J. Event-based secure H_∞ load frequency control for delayed power systems subject to deception attacks. *Appl. Math. Comput.* **2021**, *394*, 125788. [CrossRef]

28. Li, J.; Yu, T.; Zhang, X. Coordinated load frequency control of multi-area integrated energy system using multi-agent deep reinforcement learning. *Appl. Energy* **2022**, *306*, 117900. [CrossRef]
29. Civelek, Z.; GOREL, G.; Luy, M.; Barisci. N.; Cam, E. Effects on load-frequency control of a solar power system with a two-area interconnected thermal power plant and its control with a new BFA algorithm. *Elektron. Ir Elektrotechnika* **2018**, *24*, 3–10. [CrossRef]
30. Shouran, M.; Anayi, F.; Packianather, M. The bees algorithm tuned sliding mode control for load frequency control in two-area power system. *Energies* **2021**, *14*, 5701. [CrossRef]
31. Pillai, A. G.; Rita, Samuel. E. PSO based LQR-PID output feedback for load frequency control of reduced power system model using balanced truncation. *Int. Trans. Electr. Energy Syst.* **2021**, *31*, e13012. [CrossRef]
32. Zeng, H.; Zhou, S.; Zhang, X.; Wang, W. Delay-dependent stability analysis of load frequency control systems with electric vehicles. *IEEE Trans. Cybern.* **2022**, *52*, 13645–13653. [CrossRef] [PubMed]
33. Ginidi, A.; Ghoneim, S. M.; Elsayed, A.; El-Sehiemy, R.; Shaheen, A.; El-Fergany, A. Gorilla troops optimizer for electrically based single and double-diode models of solar photovoltaic systems. *Sustainability* **2021**, *13*, 9459. [CrossRef]
34. Zhong, Q.; Yang, J.; Shi, K.; Zhong, S.; Li, Z.; Sotelo, M. A. Event-triggered H_∞ load frequency control for multi-area nonlinear power systems based on non-fragile proportional integral control strategy. *IEEE Trans. Intell. Transp. Syst.* **2021**, *23*, 12191–12201. [CrossRef]
35. Chen, P.; Zhang, D.; Yu, L.; Yan, H. Dynamic event-triggered output feedback control for load frequency control in power systems with multiple cyber attacks. *IEEE Trans. Syst. Man Cybern. Syst.* **2022**, *52*, 6246–6258. [CrossRef]
36. Xu, K.; Lv, X.; Yang, Y.; Niu, Y. Load frequency secure control of interconnected power systems: Non-fragile sliding mode control strategy. In Proceedings of the 41st Chinese Control Conference, Heifei, China, 25–27 July 2022; pp. 6099–6104.
37. Yan, Z.; Xu, Y. A multi-agent deep reinforcement learning method for cooperative load frequency control of a multi-area power system. *IEEE Trans. Power Syst.* **2020**, *35*, 4599–4608. [CrossRef]
38. Kader, M. O. A.; Akindeji, K. T.; Sharma, G. A novel solution for solving the frequency regulation problem of renewable interlinked power system using fusion of AI. *Energies* **2022**, *15*, 3376. [CrossRef]
39. Wang, C.; Mi, Y.; Fu, Y.; Wang, P. Frequency control of an isolated micro-grid using double sliding mode controllers and disturbance observer. *IEEE Trans. Smart Grid* **2016**, *9*, 923–930. [CrossRef]
40. Duong, M. Q.; Grimaccia, F.; Leva, S.; Mussetta, M.; Le, K. H. Improving transient stability in a grid-connected squirrel-cage induction generator wind turbine system using a fuzzy logic controller. *Energies* **2015**, *8*, 6328–6349. [CrossRef]
41. Chojaa, H.; Derouich, A.; Taoussi, M.; Chehaidia, S. E.; Zamzoum, O.; Mosaad, M. I.; Alhejji, A.; Yessef, M. Nonlinear control strategies for enhancing the performance of DFIG-based WECS under a real wind profile. *Energies* **2022**, *15*, 6650. [CrossRef]
42. Kuppusamy, S.; Joo, Y. H.; Kim, H. S. Fault-tolerant load frequency control for DFIG-based interconnected wind power systems. *Inf. Sci.* **2022**, *582*, 73–88. [CrossRef]
43. Kim, Y.; Kang, M.; Muljadi, E.; Park, J. W.; Kang, Y. C. Power smoothing of a variable-speed wind turbine generator in association with the rotor-speed-dependent gain. *IEEE Trans. Sustain. Energy* **2016**, *8*, 990–999. [CrossRef]
44. Wang, H.; Li, Z. S. Multi-area load frequency control in power system integrated with wind farms using fuzzy generalized predictive control method. *IEEE Trans. Reliab.* **2022**. [CrossRef]
45. Sharma, G.; Panwar, A.; Arya, Y.; Kumawat, M. Integrating layered recurrent ANN with robust control strategy for diverse operating conditions of AGC of the power system. *IET Gener. Transm. Distrib.* **2020**, *14*, 3886–3895. [CrossRef]
46. Ortiz-Conde, A.; Lugo-Munoz, D.; Garcia-Sanchez, F. J. An explicit multiexponential model as an alternative to traditional solar cell models with series and shunt resistances. *IEEE J. Photovolt.* **2012**, *2*, 261–268. [CrossRef]
47. Magdy, G.; Bakeer, A.; Nour, M.; Petlenkov, E. A new virtual synchronous generator design based on the SMES system for frequency stability of low-inertia power grids. *Energies* **2020**, *13*, 5641. [CrossRef]
48. Khooban, M. H.; Gheisarnejad, M. A novel deep reinforcement learning controller based type-II fuzzy system: Frequency regulation in microgrids. *IEEE Trans. Emerg. Top. Comput. Intell.* **2020**, *5*, 689–699. [CrossRef]
49. Farooq, Z.; Rahman, A.; Lone, S. A. Load frequency control of multi-source electrical power system integrated with solar-thermal and electric vehicle. *Int. Trans. Electr. Energy Syst.* **2021**, *31*, e12918. [CrossRef]
50. Mi, Y.; Fu, Y.; Li, D.; Wang, C.; Loh, P. C.; Wang, P. The sliding mode load frequency control for hybrid power system based on disturbance observer. *Int. J. Electr. Power Energy Syst.* **2016**, *74*, 446–452. [CrossRef]
51. Qiao, S.; Liu, X.; Liang, Y.; Xiao, G.; Kang, Y.; Ge. S. S. Event-triggered sliding mode load frequency control of multi-area power systems under periodic denial-of-service attacks. *IEEE Syst. J.* **2022**, 1–12. [CrossRef]
52. Yang, F.; Shao, X.; Muyeen, S. M.; Li, D.; Lin, S.; Fang, C. Disturbance observer based fractional-order integral sliding mode frequency control strategy for interconnected power system. *IEEE Trans. Power Syst.* **2021**, *36*, 5922–5932. [CrossRef]
53. Deng, Z.; Xu, C. Frequency regulation of power systems with a wind farm by sliding-mode-based design. *IEEE/CAA J. Autom. Sin.* **2022**, *99*, 1–10. [CrossRef]
54. Mi, Y.; Song, Y.; Fu, Y.; Wang, C. The adaptive sliding mode reactive power control strategy for wind-diesel power system based on sliding mode observer. *IEEE Trans. Sustain. Energy* **2019**, *11*, 2241–2251. [CrossRef]
55. Szinai, J. K.; Sheppard, C. J.; Abhyankar, N.; Gopal, A. R. Reduced grid operating costs and renewable energy curtailment with electric vehicle charge management. *Energy Policy* **2020**, *136*, 111051. [CrossRef]
56. Ota, Y.; Taniguchi, H.; Nakajima, T.; Liyanage, K. M.; Baba, J.; Yokoyama, A. Autonomous distributed V2G (vehicle-to-grid) satisfying scheduled charging. *IEEE Trans. Smart Grid* **2011**, *3*, 559–564. [CrossRef]

57. Chatterjee, K.; Padmini, V.; Khaparde, S. A. Review of cyber attacks on power system operations. In Proceedings of the 2017 IEEE Region 10 Symposium, Cochin, India, 14–16 July 2017; pp. 1–6.
58. Li, W.; Xie, L.; Wang, Z. A novel covert agent for stealthy attacks on industrial control systems using least squares support vector regression. *J. Electr. Comput. Eng.* **2018**, *2018*, 7204939. [CrossRef]
59. De Persis, C.; Tesi, P. Input-to-state stabilizing control under denial-of-service. *IEEE Trans. Autom. Control* **2015**, *60*, 2930–2944. [CrossRef]
60. Befekadu, G. K.; Gupta, V.; Antsaklis, P. J. Risk-sensitive control under Markov modulated denial-of-service (DoS) attack strategies. *IEEE Trans. Autom. Control* **2015**, *60*, 3299–3304. [CrossRef]
61. Qiao, S.; Liu, X.; Xiao, G.; Ge, S. S. Observer-based sliding mode load frequency control of power systems under deception attack. *Complexity* **2021**, 8092206. [CrossRef]
62. Ding, D.; Han, Q. L.; Xiang, Y.; Ge, X.; Zhang, X.M. A survey on security control and attack detection for industrial cyber-physical systems. *Neurocomputing* **2018**, *275*, 1674–1683. [CrossRef]
63. Hoehn, A.; Zhang, P. Detection of covert attacks and zero dynamics attacks in cyber-physical systems. In Proceedings of the 2016 American Control Conference, Boston, MA, USA, 6–8 July 2016; pp. 302–307.
64. Ranjan, M.; Shankar, R. A literature survey on load frequency control considering renewable energy integration in power system: Recent trends and future prospects. *J. Energy Storage* **2022**, *45*, 103717. [CrossRef]
65. Sharma, J.; Hote, Y. V.; Prasad, R. Robust PID load frequency controller design with specific gain and phase margin for multi-area power systems. *IFAC-PapersOnLine* **2018**, *51*, 627–632. [CrossRef]
66. Celik, E.; Oztvrk, N.; Arya, Y.; Ocak, C. (1+ PD)-PID cascade controller design for performance betterment of load frequency control in diverse electric power systems. *Neural Comput. Appl.* **2021**, *33*, 15433–15456. [CrossRef]
67. Kumar, A.; Pan, S. Design of fractional order PID controller for load frequency control system with communication delay. *ISA Trans.* **2022**, *129*, 138–149. [CrossRef] [PubMed]
68. Puviyarasi, B.; Murukesh, C.; Alagiri, M. Design and implementation of gain scheduling decentralized PI/PID controller for the fluid catalytic cracking unit. *Biomed. Signal Process. Control* **2022**, *77*, 103780. [CrossRef]
69. Urrea-Quintero, J. H.; Fuhg, J. N.; Marino, M.; Fau, A. PI/PID controller stabilizing sets of uncertain nonlinear systems: An efficient surrogate model-based approach. *Nonlinear Dyn.* **2021**, *105*, 277–299. [CrossRef]
70. Yerolla, R.; Bestha, C. S. PI/PID controller design for critically damped SOPTD system and experimental validation. In Proceedings of the 2021 5th International Conference on Intelligent Computing and Control Systems, Madurai, India, 6–8 May 2021; pp. 531–535.
71. Sharma, P.; Mishra, A.; Saxena, A.; Shankar, R. A novel hybridized fuzzy PI-LADRC based improved frequency regulation for restructured power system integrating renewable energy and electric vehicles. *IEEE Access* **2021**, *9*, 7597–7617. [CrossRef]
72. Guha, D.; Roy, P. K.; Banerjee, S. Equilibrium optimizer-tuned cascade fractional-order 3DOF-PID controller in load frequency control of power system having renewable energy resource integrated. *Int. Trans. Electr. Energy Syst.* **2021**, *31*, e12702. [CrossRef]
73. Vigya.; Mahto, T.; Malik, H.; Mukherjee, V.; Alotaibi, M. A.; Almutairi, A. Renewable generation based hybrid power system control using fractional order-fuzzy controller. *Energy Rep.* **2021**, *7*, 641–653. [CrossRef]
74. Hou, H.; Yu, X.; Fu Z. Sliding mode control of networked control systems: An auxiliary matrices based approach. *IEEE Trans. Autom. Control* **2021**, *67*, 3574–3581. [CrossRef]
75. Liu, X.; Bai, D.; Qiao, S.; Xiao, G.; Ge, S. S. Resilient and event-triggered sliding mode load frequency control for multi-area power systems under hybrid cyber attacks. *IET Control Theory Appl.* **2022**, *16*, 1739–1750. [CrossRef]
76. Sun, Y.; Wang, Y.; Wei, Z.; Sun, Z.; Wu, X. Robust H_∞ load frequency control of multi-area power system with time delay: A sliding mode control approach. *IEEE/CAA J. Autom. Sin.* **2017**, *5*, 610–617. [CrossRef]
77. Odgaard, P. F.; Stoustrup, J.; Kinnaert, M. Fault-tolerant control of wind turbines: A benchmark model. *IEEE Trans. Control Syst. Technol.* **2013**, *21*, 1168–1182. [CrossRef]
78. Wang, C.; Li, R.; Su, X.; Shi, P. Output feedback sliding mode control of Markovian jump systems and its application to switched boost converter. *IEEE Trans. Circuits Syst. I: Regul. Pap.* **2021**, *68*, 5134–5144. [CrossRef]
79. Azizi, A.; Nourisola, H.; Shoja-Majidabad, S. Fault tolerant control of wind turbines with an adaptive output feedback sliding mode controller. *Renew. Energy* **2019**, *135*, 55–65. [CrossRef]
80. Wang, Z.; Liu, Y. Adaptive terminal sliding mode based load frequency control for multi-area interconnected power systems with PV and energy storage. *IEEE Access* **2021**, *9*, 120185–120192. [CrossRef]
81. Wang, Y.; Wang, Z.; Zou, L.; Dong, H. Non-fragile dissipative fuzzy PID control with mixed fading measurements. *IEEE Trans. Fuzzy Syst.* **2022**, *30*, 5019–5033. [CrossRef]
82. Anand, S.; Dev, A.; Sarkar, M. K.; Banerjee, S. Non-fragile approach for frequency regulation in power system with event-triggered control and communication delays. *IEEE Trans. Ind. Appl.* **2021**, *57*, 2187–2201. [CrossRef]
83. Huang, C.; Karimi, H. R. Non-fragile H_∞ control for LPV-based CACC systems subject to denial-of-service attacks. *IET Control Theory Appl.* **2021**, *15*, 1246–1256. [CrossRef]
84. Aravindh, D.; Sakthivel, R.; Kaviarasan, B.; Anthoni, S. M.; Alzahrani, F. Design of observer-based non-fragile load frequency control for power systems with electric vehicles. *ISA Trans.* **2019**, *91*, 21–31. [CrossRef]
85. Joshi, M.; Sharma, G.; Bokoro, P, N.; Krishnan, N. A fuzzy-PSO-PID with UPFC-RFB solution for an LFC of an interlinked hydro power system. *Energies* **2022**, *15*, 4847. [CrossRef]

86. Sharma, G.; Krishnan, N.; Arya, Y.; Panwar, A. Impact of ultracapacitor and redox flow battery with JAYA optimization for frequency stabilization in linked photovoltaic-thermal system. *Int. Trans. Electr. Energy Syst.* **2021**, *31*, e12883. [CrossRef]
87. Panwar, A.; Sharma, G.; Nasiruddin, I.; Bansal, R. C. JAYA-evaluated frequency control design for hydroelectric power system using RFB and UPFC. In *Intelligent Computing Techniques for Smart Energy Systems: Proceedings of ICTSES 2018*; Springer: Singapore, 2020; pp. 863–871.
88. Panwar, A.; Agarwal, V.; Sharma, G.; Sharma, S. Design of a novel AGC action for a linked hydro governing system. *Electr. Power Components Syst.* **2022**, *49*, 1201–1211. [CrossRef]
89. Sharma, G.; Panwar, A.; Krishnan, N.; Kumawat, M. Integrating LQR with GRNN for LFC of energy delivery system interconnected via AC/DC tie-lines. *IET Energy Syst. Integr.* **2020**, *2*, 355–361. [CrossRef]
90. Arya, Y.; Kumar, N.; Dahiya, P.; Sharma, G.; Celik, E.; Dhundhara, S.; Sharma, M. Cascade-$I^{\lambda}D^{\mu}N$ controller design for AGC of thermal and hydro-thermal power systems integrated with renewable energy sources. *IET Renew. Power Gener.* **2021**, *15*, 504–520. [CrossRef]
91. Yan, Z.; Xu, Y. Data-driven load frequency control for stochastic power systems: A deep reinforcement learning method with continuous action search. *IEEE Trans. Power Syst.* **2018**, *34*, 1653–1656. [CrossRef]
92. Bu, X.; Yu, W.; Cui, L.; Hou, Z.; Chen, Z. Event-triggered data-driven load frequency control for multi-area power systems. *IEEE Trans. Ind. Inform.* **2021**, *18*, 5982–5991. [CrossRef]
93. Mu, C.; Tang, Y.; He, H. Improved sliding mode design for load frequency control of power system integrated an adaptive learning strategy. *IEEE Trans. Ind. Electron.* **2017**, *64*, 6742–6751. [CrossRef]
94. Qi, X.; Zheng, J.; Mei, F. Model predictive control-based load-frequency regulation of grid-forming inverter-based power systems. *Front. Energy Res.* **2022**, *10*, 932788. [CrossRef]
95. Faragalla, A.; Abdel-Rahim, O.; Orabi, M.; Abdelhameed, E. H. Enhanced virtual inertia control for microgrids with high-penetration renewables based on whale optimization. *Energies* **2022**, *15*, 9254. [CrossRef]
96. Zhang, J.; Li, F.; Chen, T.; Cao, Y.; Wang, D.; Gao, X. Virtual inertia control parameter regulator of doubly fed induction generator based on direct heuristic dynamic programming. *Energy Rep.* **2022**, *8*, 259–266. [CrossRef]
97. Ali, H.; Magdy, G.; Li, B.; Shabib, G.; Elbaset, A. A; Xu, D.; Mitani, Y. A new frequency control strategy in an islanded microgrid using virtual inertia control-based coefficient diagram method. *IEEE Access* **2019**, *7*, 16979–16990. [CrossRef]
98. Ouyang, J.; Pang, M.; Li, M.; Zheng, D.; Tang, T. Frequency control method based on the dynamic deloading of DFIGs for power systems with high-proportion wind energy. *Int. J. Electr. Power Energy Syst.* **2021**, *128*, 106764. [CrossRef]
99. Mishra, A. K.; Mishra, P.; Mathur, H, D. A deep learning assisted adaptive nonlinear deloading strategy for wind turbine generator integrated with an interconnected power system for enhanced load frequency control. *Electr. Power Syst. Res.* **2023**, *214*, 108960. [CrossRef]
100. Hasanien, H. M.; El-Fergany, A. A. Salp swarm algorithm-based optimal load frequency control of hybrid renewable power systems with communication delay and excitation cross-coupling effect. *Electr. Power Syst. Res.* **2019**, *176*, 105938. [CrossRef]
101. Pillai, A. G.; Samuel, E. R.; Unnikrishnan, A. Optimal load frequency control through combined state and control gain estimation for noisy measurements. *Prot. Control Mod. Power Syst.* **2020**, *5*, 24. [CrossRef]
102. Zhao, X.; Zou, S.; Ma, Z. Decentralized resilient H_∞ load frequency control for cyber-physical power systems under DoS attacks. *IEEE/CAA J. Autom. Sin.* **2021**, *8*, 1737–1751. [CrossRef]